PHYSICAL REVIEW B VOLUME 11, NUMBER 12 15 JUNE 1975

Capture and emission of electrons at 2.4-eV-deep trap level in SiO_2 films*

D. J. DiMaria[†] and F. J. Feigl
Department of Physics and Materials Research Center, Lehigh University, Bethlehem, Pennsylvania 18015

S. R. Butler
Department of Metallurgy-Materials Science and Materials Research Center, Lehigh University, Bethlehem, Pennsylvania 18015
(Received 12 September 1974)

Capture, photoionization, and impact-ionization cross sections for a 2.4-eV-deep electron trapping center in the silicon-dioxide layer of a metal-oxide-semiconductor structure have been determined using the photoinjection-photodepopulation technique. The electric field dependence of both capture and impact-ionization cross sections have been determined for accelerating fields in the range 0.1–1.0 MV/cm. Capture cross sections are of order 10^{-14} cm^2 and uv photoionization cross sections greater than 10^{-18} cm^2. High-field impact-ionization rates are 1–10 cm^{-1} for filled trap densities of order 5×10^{13} cm^{-3}.

I. INTRODUCTION

Electron-capture and ionization phenomena associated with a 2.4-eV-deep trapping level in SiO_2 films produced by thermal oxidation of Si have been studied in detail. The energy and spatial distribution of this trapping level have been reported previously,[1-3] and the trapping level has been tentatively associated with sodium impurities incorporated into the SiO_2 during growth.[4] The results of the present investigation have been analyzed in terms of first-order trapping and ionization processes. The most interesting of these is hot-electron impact ionization of the filled trapping states at high applied fields. The field dependence of the impact-ionization rate has been determined from data on several samples. A preliminary report of these results has been published.[5]

II. EXPERIMENTAL DETAILS

All measurements reported herein were made on MOS (metal–silicon-dioxide-insulator–silicon-semiconductor) capacitors produced by deposition of metal electrodes onto thermally oxidized single-crystal silicon wafers. The steam-grown oxide films were 1–4 μm thick. The basic experiments executed to determine trap populations and trapping kinetics were photoinjection[1] (interfacial photoemission[6-8]) and trap photodepopulation.[1-3,6] Preparation of the MOS specimens[2,4] and instrumentation and experimental procedures for the photocurrent measurements[1-3,9] have been described in detail elsewhere. Sample characteristics are summarized in Table I.

All measurements reported below were made on MOS specimens which had been "aged" under bias by illumination with the full output of a 50-W deuterium lamp for several hours. The applied field during aging were of the order of 10^6 V/cm (metal positive with respect to silicon). The effect of aging is the introduction of negative charge in the oxide (electrons trapped at impurities and/or structural defects).[10]

The important characteristic of aged specimens was that the photoemission characteristic curve [curve (b) of Fig. 1] was stable against further aging. This indicated that a steady-state trap population had been attained. The negative charge associated with the 2.4-eV-deep electron trapping state is typically only 1% of the total negative space charge produced in the insulator by the aging process. The charge in the 2.4-eV-deep trapping-state distribution could be removed by illumination of the sample with visible light (450-nm central wavelength, 20-nm bandpass) under bias.

The transport sequence examined in the present investigation was[5] (i) uv-excited electron transport and proportionate electron capture into a 2.4-eV-deep electron trapping level *(photoinjection)*, and (ii) subsequent visible photon-stimulated emptying of these traps and counting of the released charge *(photopopulation)*. The primary object of these measurements was systematic determination of the population of the 2.4-eV-deep trapping level as a function of the experimental variables in the photoinjection process (applied voltage, uv light intensity, and time cf photoinjection). This trap population is expressed as $q(t)$, the trapped charge density after uv photoinjection for time t.

In order to determine $q(t)$, photodepopulation measurements were made at a depopulating light wavelength of 450 nm and at both high positive

TABLE I. MOS samples used in present investigation.

Sample No.	Silicon resistivity [a] (Ω cm)	Oxide thickness [b] (μm)	Electrode metal [c]
BTL1	0.001	3.6	Au
BTL2	0.001	2.4	Ni
LU11	5	1.1	Al

[a]All substrates were (100) *n*-type silicon wafers.
[b]Oxide thickness was determined by high-frequency capacitance and optical interference measurements.
[c]Electrode thickness was of order 10 nm.

and high negative applied fields (i.e., in both the negative-bias and positive-bias saturated collected-charge regions of the photodepopulation Q-V characteristic curve[9]). From these data, both the total trapped charge and its centroid after photoinjection for time t could be determined.[9] The centroid of the spatial distribution of charge trapped in the 2.4-eV state distribution was approximately 0.5 in all samples investigated, and did not change through the execution of the experiments described herein. Analytical expressions for determining $q(t)$ and its spatial centroid from photodepopulation measurements are found in DiMaria and Feigl.[9] As noted previously,[5] periodic checks of the complete wavelength and voltage dependence of the photodepopulated charge were made. These data indicated that neither the energy distribution nor the spatial distribution of trapping states emptied by visible radiation varied throughout the measurement program.

III. EXPERIMENTAL RESULTS

As mentioned above, stimulation of internal photoemission by uv illumination of as-grown MOS specimens caused a buildup of negative charge within the insulating layer. The influence of this charge on MOS photoemission characteristics is exhibited in Fig. 1. The response of the as-deposited sample [curve (a)] was as reported by Powell and Berglund: an emission-limited characteristic curve determined by scattering of photoexcited electrons in the image force potential well near the emitting Si-SiO_2 interface.[7,11] The effective scattering length determined by fitting data for several samples was approximately 30 Å, in excellent agreement with previous results.[7] These data indicated that in the as-deposited oxide films, any significant insulator charge was located in the immediate vicinity of either the Si-SiO_2 or the SiO_2-metal interface.[11] The photoemission response in the specimen after aging [curve (b)] was that characteristic of a large negative space charge in the oxide film. For high fields, resulting in normalized currents greater than 5×10^{-9} A/mW cm^{-2} for the data of Fig. 1, curve (b), the photoemission characteristic curve is laterally translated from that of the as-deposited film. The curvature at low fields [normalized currents less than 5×10^{-9} A/mW cm^{-2}, curve (b)] can be related at least in part to the detailed spatial variation of trapped negative charge near the emitting interface.[7] The low-field photoemission characteristic may also be determined by lateral charge or emission inhomogeneities.[12,13] These phenomena were not systematically addressed during the present investigation, since only the high-field region was of interest. This will be discussed further in Sec. IV. At any given applied field, the photoinjection current measured on an aged specimen was proportional to the uv light intensity during photoinjection. Selected data is exhibited in Fig. 2.

Figure 3 exhibits the results of photoinjection-photodepopulation measurements on an aged MOS specimen. The solid lines represent weighted statistical best fits of the data to a first-order kinetic function:

$$q(t)=q(\infty)(1-e^{-t/\tau}), \qquad (1)$$

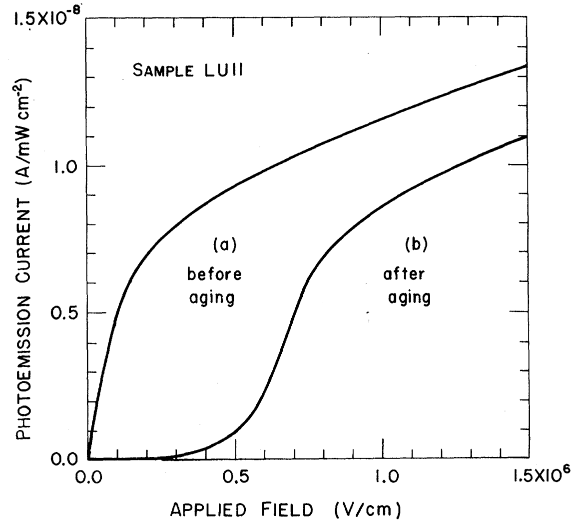

FIG. 1. Photoemission characteristic curves (current vs applied field) for electron emission from the silicon–silicon-dioxide interface of an MOS capacitor. The two curves were obtained on a single capacitor (a) as fabricated (1.1-μm-thick steam-grown oxide with Al electrode) and (b) after uv illumination for several hours with metal electrode positive (applied field approximately 10^6 V/cm). The photocurrent is normalized to the incident light intensity during measurement. The incident light intensity during measurement of photoemission characteristics of the unaged capacitor was approximately 1% of that during aging.

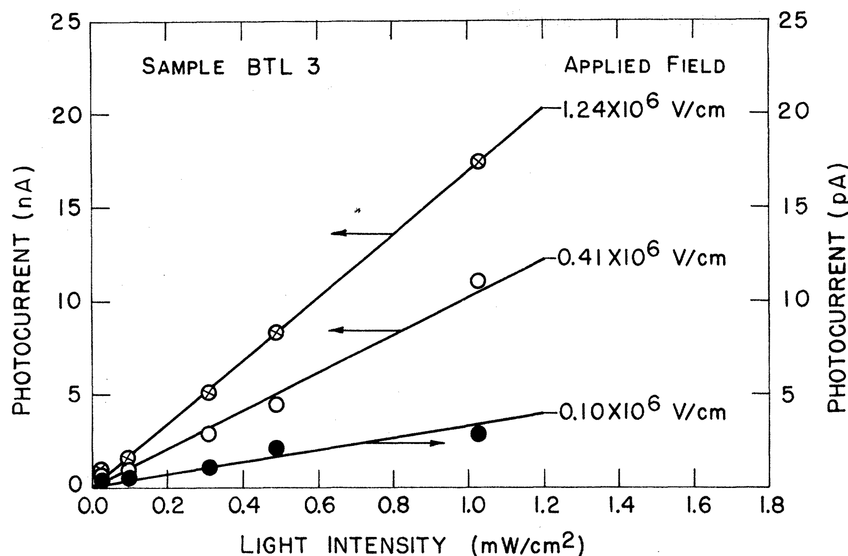

FIG. 2. uv-stimulated photoemission current as a function of uv light intensity during photoinjection, for different applied fields.

where $q(\infty)$ is the steady-state trapped charge density, and τ is the trap-filling time constant.

At any given applied field, the photoinjection current (cf. Fig. 2) and consequently the trap-filling rate were proportional to S, the uv light intensity during photoinjection. Selected data on $q(\infty)$ and τ are exhibited in Table II. Both the steady-state trapped charge density and the normalized trapping rate k/S are independent of S to within the accuracy of the measurements.

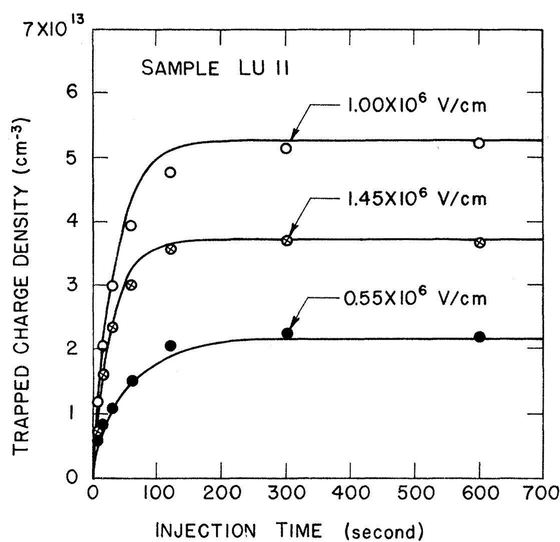

FIG. 3. Insulator bulk averaged trapped charge density (total charge/insulator volume) as a function of photoinjection time, for different applied fields during photoinjection. The ordinate refers to charge injected into the 2.4-eV-deep trapping-state distribution in the insulator.

$k \equiv \tau^{-1}$ is the trap-filling rate.

The variation of steady-state trapped charge density $q(\infty)$ with applied field during photoinjection is exhibited for three aged samples in Fig. 4. As noted previously,[5] the most interesting feature of these data was the decrease of steady-state trapped charge density with increasing fields in the region of high applied fields (around 10^6 V/cm). This decrease was attributed to field-accelerated electron impact ionization of filled traps.[5]

IV. ANALYSIS

The kinetics of electron population of the 2.4-eV-deep trapping state in thermal SiO_2 films were analyzed in terms of a first-order kinetic rate equation:

$$\frac{dq(t)}{dt} = n v_T \sigma_e [eN - q(t)] - S\sigma_P q(t) - n v_T \alpha q(t) . \tag{2}$$

TABLE II. Variation of trapped charge with light intensity during photoinjection. (Data obtained on sample BTL2 with an applied field of 6.2×10^5 V/cm during photoinjection.)

S (mW/cm^2)	τ (sec)	k/S (cm^2/mW-sec)	$q(\infty)/e$ (10^{13} cm^{-3})
0.03	462	0.072	3.1
0.10	140	0.074	3.3
0.31	49	0.069	3.4
1.03	15	0.063	3.6

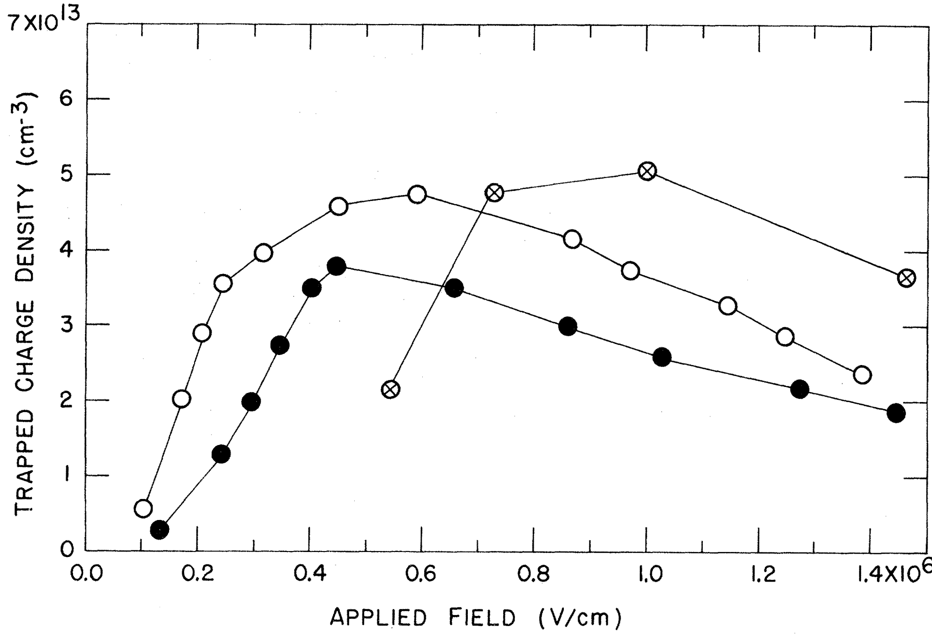

FIG. 4. Steady-state bulk averaged trapped charge density $[q(\infty)/e]$ as a function of applied field during photoinjection for three specimens: BTL1 (open circles), BTL2 (solid circles), LU11 (crossed circles). The lines in the drawing are for purposes of visualization only.

N is the average density of trapping centers in the oxide film (number of traps per cm^3), n is the conduction-electron density, and v_T is the thermal velocity of a conduction electron. σ_e is the electron capture cross section of the trapping centers, σ_P is the ultraviolet photoionization cross section, and α is a high-field electron-impact-ionization cross section. Because of the depth of the trap relative to kT at room temperature, thermal-ionization effects have been neglected.[14]

If it is assumed that applied fields during photoinjection are large enough so that the drift velocity of the conduction electrons is saturated at its thermal value, or, equivalently, that the conduction electrons travel in approximately straight lines across the insulator; then the current density during photoinjection is $J = I/A \approx env_T$. I is the external-circuit current during photoinjection, A is the active electrode area, and e is the electronic charge. This assumption has been verified by previous investigators.[6,15] For aged specimens, the photoinjection currents were demonstrated to be constant in time (see Sec. III). The 2.4-eV-deep oxide traps were emptied of charge by photodepopulation prior to each photoinjection sequence in Fig. 3. Under these conditions, Eq. (1) is a solution of the differential equation (2), with

$$q(\infty) = eN\left(1 + \frac{eS}{J}\frac{\sigma_P}{\sigma_e} + \frac{\alpha}{\sigma_e}\right)^{-1} \tag{3}$$

and

$$\tau = (nv_T\sigma_e + S\sigma_P + nv_T\alpha)^{-1} = \frac{e}{J\sigma_e}\frac{q(\infty)}{N}. \tag{4a}$$

Several mechanisms could be responsible for the observed high-field decrease in $q(\infty)$ (see Figs. 3 and 4). Field-assisted Poole-Frenkel or tunneling emission of charge from the trapping states was ruled out by direct experimental test. Without current flow, trapped-charge removal by applied-field stressing was negligible within experimental error. Powell has demonstrated that hole currents are negligible under photoinjection conditions.[16] Electron-hole recombination effects were therefore presumed negligible.[17] Since the energy of the photoexciting light was far above the 2.4-eV trap threshold, σ_P was assumed to be independent of applied field.[18,19] The data of Fig. 4 were reproducible, and *reversible*. Thus, the total density of trapping states N was presumed constant for a given aged MOS specimen. The final mechanisms appropriate to the observed results are electron impact ionization of the occupied traps[20-22] and variation of the electron capture cross section σ_e with applied field.[21,23]

Photoemission characteristics are plotted for the three different aged MOS specimens used in this study in Fig. 5. The vertical scale is arbitrary,[24] and the horizontal axis is normalized by subtracting an effective retarding field associated with the space-charge buildup during aging of each sample. The effective retarding field was obtained by a graphical fit of data for each aged

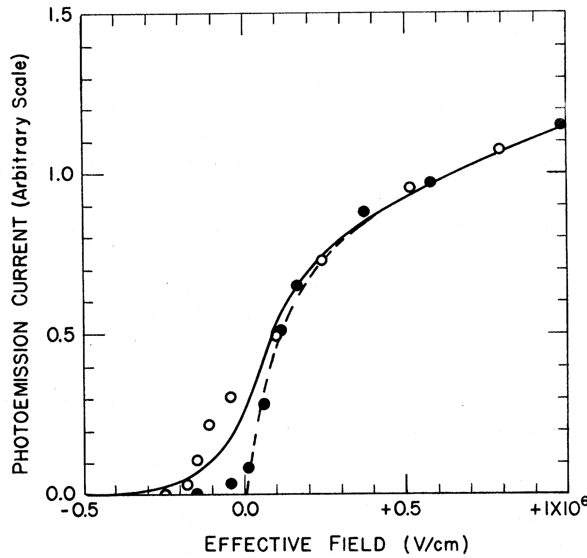

FIG. 5. Normalized photoemission characteristic curves (current vs effective accelerating electric field) for three aged MIS specimens: BTL1 (open circles), BTL2 (solid circles), LU11 (solid line). The dash line represents direct photoemission characteristics for an unaged specimen [LU11—see Fig. 1, curve (a)]. The ordinate scaling factors relative to LU11 are 0.75 for BTL1 and 1.80 for BTL2. These are multiplicative factors for current which can be interpreted as a relative photoemission efficiency (see Ref. 24). The abscissa corrections relative to unaged LU11 are −0.62 MV/cm for LU11, −0.32 MV/cm for BTL1, and −0.25 MV/cm for BTL2. These last are additive factors which can be interpreted as effective space-charge retarding fields (see text).

sample to the uncorrected high-field photoemission characteristic of a charge-free unaged MOS specimen [the broken curve in Fig. 5 and the data of Fig. 1(a)]. In effect, Fig. 5 displays the photoemission current variation with net accelerating field in the oxide film.

Numerical values for σ_e and α were obtained by a two-step fit of the data of Figs. 3–5 and Table II. First, the product $N\sigma_e$ was obtained using Eq. (4a) in the form

$$N\sigma_e = e\frac{1}{J}\frac{q(\infty)}{\tau}. \tag{4b}$$

$q(\infty)$, τ, and J are experimentally determined quantities (Fig. 3 and Table II, and Fig. 5).

Second, using these values of $N\sigma_e$, the data of Fig. 4 were fit by the method of least squares to Eq. (3) and a conventional phenomenological form[20,22,25] of the impact-ionization cross section α:

$$\alpha = \alpha_\infty e^{-b/E'_a}, \quad E'_a > 0. \tag{5}$$

In Eq. (5), α_∞ and b are empirical parameters and E'_a is the effective accelerating field in the insulator, as previously defined (see Fig. 5). The results of the fitting procedure are displayed in Figs. 6–8 and Table III. In Fig. 6, the trap occupancy fraction $q(\infty)/N$ is displayed for three aged MOS specimens as a function of accelerating field E'_a. In Fig. 7, the variation of electron capture cross section σ_e with accelerating field E'_a is displayed for the three MOS specimens. Weighted average values from the fit to data displayed in Fig. 6 for photoionization cross section σ_P and impact-ionization parameters α_∞ and b are listed in Table III. Figure 8 shows the variation of the impact-ionization cross section α with accelerating field E'_a.

V. DISCUSSION

In summary, Figs. 6–8 display the variation of fractional trap occupancy, electron capture cross section, and impact-ionization cross section with effective accelerating field in thermal SiO_2 films. We conclude that hot-electron impact ionization[26] is the cause of the reduction of the fractional trap occupancy with increasing positive accelerating field. The photon-flux spectrum of the uv photoexcitation source used in these experiments was a relatively broad distribution with maximum output well above the silicon-valence-band–silicon-dioxide-conduction-band internal photoemission threshold (peak at 5.5 eV, half-width at half-maximum 0.75 eV). The energy distribution of mobile electrons admitted into the biased insulator volume thus includes a significant fractional component with kinetic energy well above thermal values and momentum normal to the emitting interfact (of order 10% between 1 and 2 eV for the step or ramp distributions cited by

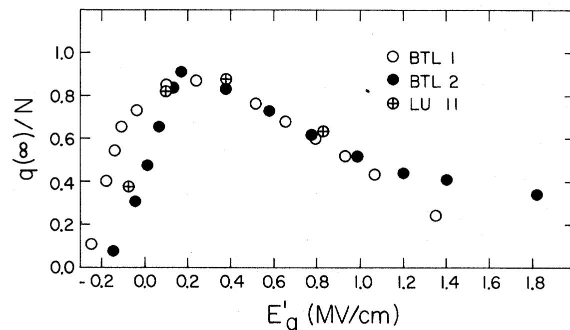

FIG. 6. Fractional trap occupancy $q(\infty)/N$ vs effective field E'_a for three different aged samples. The best-fit bulk averaged trapping-state density N for each sample was 5.42×10^{13} cm^{-3} for BTL1, 4.24×10^{13} cm^{-3} for BTL2, and 5.82×10^{13} cm^{-3} for LU11.

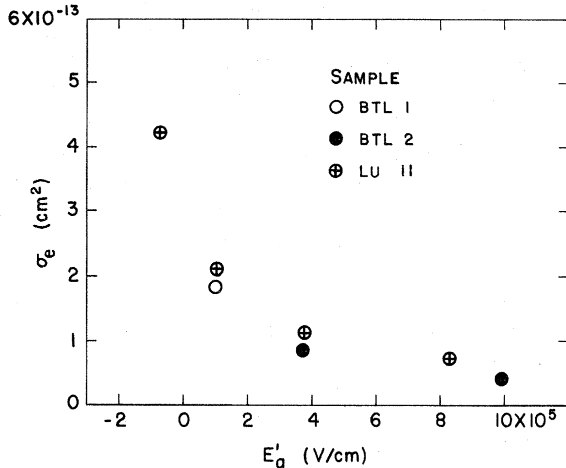

FIG. 7. Best-fit capture cross section σ_e vs effective field E_a' for three different aged samples.

Powell[27]). The results and conclusion just cited, and the trap ionization parameters listed in Table III, apply to this entering-electron distribution.

From Eqs. (3) and (4), the trap population process can be characterized by the following expression for the trap-filling rate:

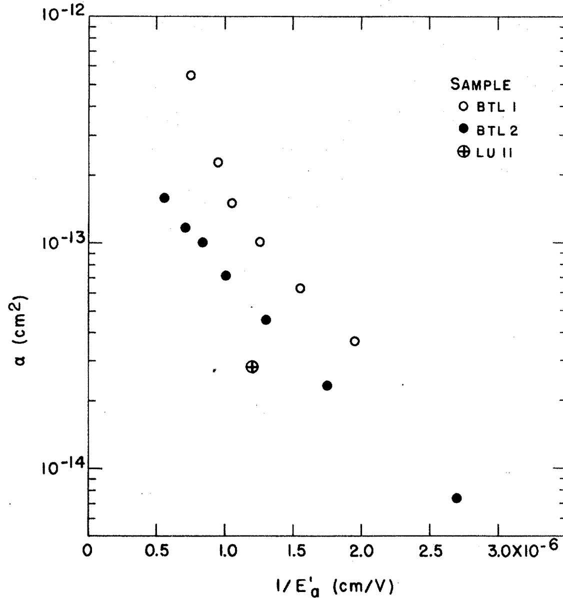

FIG. 8. Variation of impact-ionization cross section with effective field E_a' for three different aged samples. For effective fields greater than 1.2×10^6 V/cm ($1/E_a'$ less than 0.8), the error in data was significant due to prebreakdown effects indicated by significant changes in dark-current characteristics.

$$k=\frac{J}{e}\sigma_e+S\sigma_p+\frac{J}{e}\alpha\,. \tag{6}$$

Within the framework of this first-order kinetic relation, we have reached the following specific conclusions from the data of Figs. 6–8 and Table III regarding electron capture and ionization of the 2.4-eV-deep trap in thermal SiO_2 films.

(i) At low effective applied fields ($0<E_a'<0.1$ MV/cm), the second term in Eq. (6) is dominant, and trapping kinetics are limited by uv photoionization. The value of σ_p, the uv photoionization cross section determined from the data-fitting procedure described in Sec. IV, is the same order of magnitude as visible photoionization cross sections for the 2.4-eV-deep trapping-state distribution. The latter cross sections were determined[28] from the time dependence of photodepopulation currents produced by narrow-band visible light (0.1-eV bandpass at several photon energies between 2 and 3 eV).

(ii) At intermediate effective fields (E_a' between 0.1 and 0.3 MV/cm), the first term of Eq. (6) is dominant. This means that $J\sigma_e$ is large compared to $eS\sigma_p$ and $J\alpha$, and thus that most of the traps are filled [cf. Eq. (3) and Fig. 6]. The largest capture cross section determined was $\sigma_e=4\times10^{-13}$ cm² (Fig. 7). This is a factor of 10 less than that anticipated for a singly charged unscreened Coulomb-attractive center in SiO_2.[23,26] The dependence of σ_e on E_a' (see Fig. 7) is similar to that determined by Sah and co-workers for ionized sulfur centers in silicon.[21,23] The high-field value of $\sigma_e\approx1\times10^{-13}$ cm² appears too high by two orders of magnitude for a neutral point defect, and too high for an aggregate center (the diameter is 10 Si-O bond lengths). We conclude that the data of Fig. 7, within the context of our assumptions regarding internal fields and mobile-electron energy distribution in the insulator (discussed below), indicate that the 2.4-eV trap level is associated with a Coulomb-attractive defect.[29] The capture rate at high fields is $\sigma_eN\approx5$ cm⁻¹. For a 2-μm-thick oxide, 5 in 10^4 conduction electrons photoinjected into the oxide would be captured into a half-filled trap distribution. The capture cross sections agree with recent results of Ning, Yu, and Osburn.[30]

(iii) At high effective fields (E_a' greater than

TABLE III. Best-fit values of ionization parameters for 2.4-eV-deep electron trap in thermal SiO_2 films.

σ_P	4.2×10^{-18} cm²
α_∞	4.9×10^{-13} cm²
b	1.5×10^{6} V/cm

0.4 MV/cm), the last term in Eq. (6) becomes important. As noted previously,[5] the infinite-field ionization rate $\alpha_\infty N \approx 25\ cm^{-1}$, when scaled for electron-density differences, is several orders of magnitude greater than that determined for band-to-band excitations in semiconductors.[20] The impact-ionization parameter $b = 1.5$ MV/cm is half that determined for a 2-eV-deep trapping level associated with Mn impurities in ZnSe.[22] The data of Fig. 6 indicate that the impact-ionization rate must equal the electron capture rate at an applied field of 1 MV/cm. At this field in a 2-μm oxide, 5 in 10^4 conduction electrons must be involved in an Auger ionization of a 2.4-eV trap (assuming a half-filled trap distribution).

The electron capture process and the impact-ionization or Auger-ionization process must involve different components of the conduction-electron distribution in the oxide film, as discussed below.

It is reasonable to assume that the major fraction of photoinjected electrons are rapidly thermalized within the oxide,[31] and that the capture process involves these electrons. The ionization process, however, must involve electrons with kinetic energy exceeding the trap depth. Examination of the internal photoemission spectrum[17,27,32] indicates that the number of electrons admitted into the oxide with such energies is not sufficient to account for the high-field data in Fig. 6. Thus, high-field acceleration of electrons to sufficient energy to participate in Auger ionization of the 2.4-eV traps must be assumed. The assumption that this involves *initially thermalized* electrons is problematic. The statistical fraction of such electrons which can be accelerated to energies well above the trap depth is insignificant, if reasonable[11,15,29] scattering lengths are used (1–3 nm, or less).

It is thus probable that impact ionization of the 2.4-eV-deep traps involves the significant fraction of photoexcited electrons which enter the oxide with kinetic energies well above thermal values. This would mean that such electrons are unstable against thermalization (optical-phonon processes) at fields of order 1 MV/cm. Since this is a runaway process, it could lead to interband Auger processes, and current runaway, at least in thicker oxides (10–100 μm).

It is clear that further detailed studies of the impact-ionization process as a function of temperature and of the energy distribution of the photoinjected electrons (i.e., of the energy spectrum of the uv photoemission source) could provide important information on electron dynamics in amorphous silica. In particular, the existence of a threshold for trap ionization at electron energies less than the trap depth, implicit in the above discussion, should be investigated. Such studies, building on the analytical procedure developed in this study, would be greatly simplified by use of the ac experimental techniques developed by Thomas for measuring photodepopulation currents.[33]

The experimental and analytical procedure developed in this study should be a powerful tool for studying trapping processes in other metal-insulator-metal or metal-insulator-semiconductor structures. The over-all logic is similar to that developed by Sah for study of trapping phenomena in semiconductor junctions, using current and capacitance data.[34] The basic techniques have been applied to Al_2O_3,[35,36] and Ta_2O_5.[33] It should be emphasized that careful measurement and detailed analysis of the current-injection characteristic of the insulator under investigation is essential to any such study. In the present case, the extensive and systematic research program of Powell and co-workers[7,8,11,27] was such a basis.

ACKNOWLEDGMENTS

The authors would like to acknowledge the extensive experimental assistance of Dr. Yusuke Ota. The assistance of Professor Garold Borse and Dr. Kenneth Klenk is also appreciated. Useful critical conversations were held with C. N. Berglung, T. H. DiStefano, N. Klein, M. Lampert, P. Mark, and C. T. Sah. One of the authors (F. J. F.) was supported in this research by the U. S. Navy Office of Naval Research.

---

*Research supported in part by National Science Foundation Engineering Materials Division Grant No. GK29113. Based in part on a dissertation submitted by D. J. DiMaria to Lehigh University.

†National Science Foundation Trainee. Present address: IBM Thomas J. Watson Research Center, Yorktown Heights, N.Y. 10598.

[1]J. H. Thomas and F. J. Feigl, Solid State Commun. 8, 1669 (1970); J. Phys. Chem. Solids 33, 2197 (1972).
[2]J. H. Thomas, J. Appl. Phys. 44, 811 (1973).
[3]F. J. Feigl, D. J. DiMaria, and J. L. Vorhaus, Bull. Am. Phys. Soc. 18, 584 (1973).
[4]Y. Ota and S. R. Butler, Bull. Am. Phys. Soc. 18, 584 (1973); J. Electrochem. Soc. 121, 1107 (1974).

[5]D. J. DiMaria, F. J. Feigl, and S. R. Butler, Appl. Phys. Lett. 24, 459 (1974); Bull. Am. Phys. Soc. 18, 584 (1973).
[6]R. Williams, Phys. Rev. 140, A569 (1965).
[7]C. N. Berglund and R. J. Powell, J. Appl. Phys. 42, 574 (1971).
[8]R. J. Powell, IEEE Trans. Nucl. Sci. NS-17, 41 (1970).
[9]D. J. DiMaria and F. J. Feigl, Phys. Rev. B 9, 1874 (1974).
[10]E. H. Nicollian, C. N. Berglund, P. F. Schmidt, and J. M. Andrews, J. Appl. Phys. 42, 5654 (1971).
[11]R. J. Powell and C. N. Berglund, J. Appl. Phys. 42, 4390 (1971).
[12]T. H. DiStefano, Appl. Phys. Lett. 19, 280 (1971); J. Appl. Phys. 44, 527 (1973). See also R. Williams and M. H. Woods, *ibid.* 43, 4142 (1972).
[13]J. R. Brews, J. Appl. Phys. 44, 379 (1973). See also J. R. Brews and A. D. Lopez, Solid-State Electron. 16, 1267 (1973).
[14]M. Lampert and P. Mark, *Current Injection in Solids* (Academic, New York, 1970), pp. 146 and 147.
[15]A. M. Goodman, Phys. Rev. 164, 1145 (1967); P. C. Hughes, Phys. Rev. Lett. 30, 1333 (1973).
[16]R. J. Powell, J. Appl. Phys. 40, 5093 (1969).
[17]It has recently been suggested that low hole-current-to–electron-current ratios may correlate with high hole-density–to–electron-density ratios during current injection in insulators. However, the strong field dependence needed to account for present observations is not anticipated by these considerations. See J. J. O'Dwyer, Bull. Am. Phys. Soc. 18, 584 (1973).
[18]L. L. Rosier and C. T. Sah, J. Appl. Phys. 42, 4000 (1971).
[19]G. Lucovsky, Solid State Commun. 3, 299 (1965).
[20]J. L. Moll, *Physics of Semiconductors* (McGraw-Hill, New York, 1964), Chaps. 10 and 11.
[21]L. L. Rosier and C. T. Sah, Solid-State Electron. 14, 41 (1971).
[22]A. W. Livingstone and J. W. Allen, J. Phys. C 6, 3491 (1973).
[23]G. A. Dussel and K. W. Boer, Phys. Status Solidi 39, 375 (1970).
[24]The photoemission efficiency of Si surfaces in metal-insulator-semiconductor specimens have been shown to be strongly dependent on the chemical purity of the Si-SiO_2 interference, particularly with respect to sodium density and distribution. See T. H. DiStefano, Appl. Phys. Lett. 19, 280 (1971).
[25]N. Klein, Adv. Phys. 21, 605 (1972).
[26]R. H. Bube, *Electronic Properties of Crystalline Solids* (Academic, New York, 1974).
[27]R. J. Powell, J. Appl. Phys. 41, 2424 (1970).
[28]D. J. DiMaria, dissertation (Lehigh University, 1973) (unpublished).
[29]T. H. DiStefano and K. N. Tu, National Technical Information Service, Arlington, Va., Report No. AFCRL-TR-74-0194, 1974 (unpublished). T. H. DiStefano (private communication) has pointed out that the interpretation of capture cross-section magnitudes in the context of average fields and average electron velocities is ambiguous. Reduced internal fields may be produced by nonmobile positive charges (see above report). In this case, the capture-cross-section data of Fig. 7 could be consistent with an electron trap that is negative when occupied.
[30]T. H. Ning and H. N. Yu, J. Appl. Phys. 45, 5373 (1974); T. H. Ning, C. M. Osburn, and H. N. Yu, Appl. Phys. Lett. 26, 248 (1975).
[31]Z. A. Weinberg, W. C. Johnson, and M. A. Lampert, Appl. Phys. Lett. 25, 42 (1974).
[32]A. M. Goodman, Phys. Rev. 152, 785 (1966).
[33]J. Thomas, Appl. Phys. Lett. 22, 406 (1973); J. Appl. Phys. 45, 835 (1974).
[34]C. T. Sah, L. Forbes, L. L. Rosier, and A. F. Tasch, Jr., Solid-State Electron. 13, 759 (1970). A recent comprehensive review of this work is given in C. T. Sah, Solid State Electronics Laboratory, University of Illinois, Urbana, Technical Report No. 26, 1973 (unpublished).
[35]D. Mehta, S. R. Butler, and F. J. Feigl, J. Appl. Phys. 43, 4631 (1972); J. Electrochem. Soc. 120, 1707 (1973).
[36]E. Harari and B. S. H. Royce, Appl. Phys. Lett. 22, 106 (1973).